

## ARTIFICIAL INTELLIGENCE–ASSISTED DIGITAL HISTOPATHOLOGICAL DETECTION OF CANCER STEM CELL NICHES IN ORAL SQUAMOUS CELL CARCINOMA

Muhammad Zulfiqah Sadikan<sup>1</sup>, Ambreen Rehman<sup>2</sup>, Syed Tahir Husain<sup>3</sup>, Faham Nehal<sup>4</sup>, Muhammad Omer Afzal Bhatti<sup>5</sup>, Seema Shafiq<sup>6</sup>, Rabail Khero<sup>7</sup>

<sup>1</sup>Faculty of Pharmacy and Health Sciences, University Kuala Lumpur Royal College of Medicine Perak, Jalan Greentown, 30450 Ipoh, Perak, Malaysia

<sup>2</sup>Assistant Professor, Department of Oral Biology, Fujairah University, UAE

<sup>3</sup>Consultant (Assistant Professor), Liaquat National Hospital, Karachi, Pakistan

<sup>4</sup>Dental Officer, Darul Sehat Hospital and Liaquat College of Medical and Dental Sciences, Karachi, Pakistan

<sup>5</sup>MBBS, MCPS, Lecturer Radiology, Department of Surgery, College of Medicine, Northern Border University, Arar, Saudi Arabia

<sup>6</sup>Assistant Professor, Oral Pathology, Islamic International Dental College & Hospital, Riphah International University, Islamabad, Pakistan

<sup>7</sup>Dentist / MD Resident, Oral Pathology Department, Liaquat College of Medicine and Dentistry, Karachi, Pakistan

\*Corresponding Author: Ambreen Rehman, Email: drambreenrehman@gmail.com

### ABSTRACT

**Background:** Cancer stem cells play an important role in tumor progression, invasion, metastasis, and treatment resistance in oral squamous cell carcinoma. Artificial intelligence–assisted digital histopathology offers a promising approach for automated detection of complex tumor microenvironmental patterns, including cancer stem cell niches.

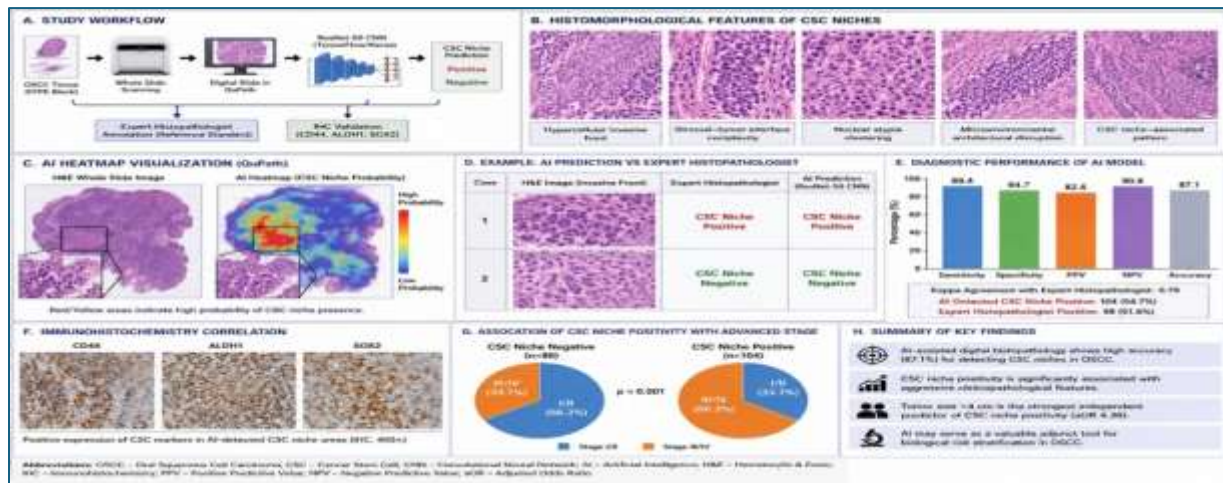
**Objective:** To evaluate the diagnostic performance and clinicopathological correlation of artificial intelligence–assisted digital histopathological detection of cancer stem cell niches in oral squamous cell carcinoma

**Methods:** This cross-sectional analytical study was conducted at AI-assisted digital histopathology labs across Karachi, from March 2023 to September 2025, including 190 patients with histopathologically confirmed oral squamous cell carcinoma.

**Results:** The mean age was  $54.2 \pm 11.8$  years, with 69.5% males. AI-assisted analysis demonstrated sensitivity of 89.4%, specificity of 84.7%, positive predictive value of 82.6%, negative predictive value of 90.8%, and overall diagnostic accuracy of 87.1%, with strong agreement with expert histopathologists ( $\kappa = 0.79$ ). AI-detected CSC niches were identified in 104 (54.7%) patients and were significantly associated with larger tumor size ( $4.4 \pm 1.4$  vs.  $3.1 \pm 1.2$  cm;  $p < 0.001$ ), lymph node metastasis (60.6% vs. 26.7%), poorly differentiated histology (36.5% vs. 12.8%), perineural invasion (40.4% vs. 18.6%), and advanced pathological stage (66.3% vs. 33.7%). Tumor size  $>4$  cm was the strongest independent predictor of CSC niche positivity (aOR 4.36;  $p < 0.001$ ).

**Conclusion:** Artificial intelligence–assisted digital histopathology demonstrates strong diagnostic performance for cancer stem cell niche detection and shows significant correlation with aggressive clinicopathological features in oral squamous cell carcinoma.

**KEYWORDS:** Oral squamous cell carcinoma; artificial intelligence; digital pathology; cancer stem cells; computational histopathology; tumor microenvironment.



## INTRODUCTION

Oral squamous cell carcinoma (OSCC) ranks among the most prevalent malignancies of the head and neck region, with its aggressive biological characteristics and often local invasion being responsible for the high recurrence rate and very modest long-term survival rates, making it a significant public health problem worldwide [1]. It is responsible for the majority of oral cancers, and is especially common in South Asian countries, where these risk factors play a major role in the burden of the disease [2]. Although the surgical treatment of cancer and the use of adjuvant therapy has improved, recurrence and therapeutic resistance are still a big problem in clinical practice [3]. The evidence on the role of cancer stem cells (CSCs) in the initiation, progression, invasion, metastasis, resistance to therapy, and recurrence of OSCC is growing and warrants the consideration that these cells are central players in OSCC. Cancer stem cells are a distinct subset of tumour cells endowed with self-renewal properties, pluripotency-like characteristics and the capacity to restore the heterogeneous tumour cell population [5]. It is believed these cells play a disproportionate role in the aggressiveness of the tumor and failure of conventional therapy. The cancer stem cell niche, or the tumor environment around cancer stem cells, is important to maintain cancer stemness, support immune evasion, drive epithelial-mesenchymal transition, and help increase metastatic potential [6]. Thus, identification of CSC niches histopathologically may yield useful prognostic and biological information. Nevertheless, classical microscopic assessment is subjective, interobserver variable, and difficult to achieve subtle architectural and cellular patterns of CSC-containing areas [7]. The whole-slide imaging of digital histopathology has revolutionized pathological diagnosis by providing standardization of image interpretation, computational analysis and remote diagnosis [8]. Recently, artificial intelligence (AI), more specifically machine learning and deep learning algorithms, has demonstrated excellent potential to analyze histopathological images for cancer detection, grading, segmentation, identification of cancer biomarkers, and prediction of prognosis in cancer [9]. AI in pathology presents opportunities for increased reproducibility, faster analysis and the identification of microstructural features which may be more challenging to quantify manually.

In the context of OSCC, the use of AI-based histopathological analysis for tumor classification, grading, invasion front analysis, prediction of lymph node metastasis, and outcome modelling have been increasingly explored [10]. This application is being expanded to include detection of histomorphological niches associated with CSC, which is an emerging and clinically relevant application [11]. The pathological characterization of AI-driven recognition of CSC-enriched microenvironments could improve and potentially be furthered by biological risk stratification. CD44, ALDH1, SOX2, OCT4, NANOG and other stemness markers have been linked to CSC populations in OSCC [12]. Computational histopathological analysis, however, when combined with digital pathology, could offer further insights beyond individual biomarker quantification, in determining niche architecture [13]. More precise tumor phenotyping could be achieved with the assistance of automated recognition of complex microenvironmental patterns. While the accuracy of AI systems in oral cancer histopathology has been shown to improve over time, the focused research on cancer stem cell niche detection is still relatively limited [14, 15].

## Objective

To evaluate the diagnostic performance and clinicopathological correlation of artificial intelligence–assisted digital histopathological detection of cancer stem cell niches in oral squamous cell carcinoma.

## METHODOLOGY

This was a cross-sectional analytical study conducted at AI-assisted digital histopathology labs across Karachi, from March 2023 to September 2025, including 190 patients with histopathologically confirmed oral squamous cell carcinoma. Patients over 18 years old who had histopathologically confirmed primary oral squamous cell carcinoma and sufficient fixed paraffin embedded tissues for digital histopathological examination were included. Cases that were eligible included those with full clinicopathological data, an adequate amount of tissue for image digitisation and computational evaluation, and diagnostic histology slides. Patients with recurrent oral squamous cell carcinoma, previous neoadjuvant chemotherapy or radiotherapy that drastically altered the tumor histomorphology, metastatic lesions from non-oral primary tumors, inadequate histopathological records, and images of digital slide analysis that were too weak to be used for AI were excluded.

## Data Collection

Thereafter, ethical approval was obtained and the data were elicited by a structured proforma. The clinicodemographic variables included in the analyses were age, sex, history of tobacco exposure, betel nut exposure, site of the tumor, duration of the lesion, size of the tumor, nodal status, histological grade, presence of lymphovascular invasion, perineural invasion, and pathological stage. Whole-slide digital imaging systems were used to digitize histopathological slides and produce standardized high-resolution digital images. The digitized slides were analyzed using QuPath digital pathology software integrated with a deep learning convolutional neural network model based on ResNet-50 architecture and developed through a TensorFlow/Keras backend. The artificial intelligence model was

used for automated detection of cancer stem cell niche-associated histomorphological patterns, including hypercellular invasive fronts, stromal-tumor interface complexity, nuclear atypia clustering, microenvironmental architectural disruption, and CSC-associated spatial pattern organization. Different histomorphological features linked to cancer stem cell niches were assessed by artificial intelligence-assisted image analysis by applying a computational pathology framework trained with a validated deep learning algorithm that allows identification of: (1) hypercellular invasive fronts, (2) stromal-tumor interface complexity, (3) nuclear atypia clustering, (4) architecture of the microenvironment, and (5) CSC-associated spatial pattern recognition. Immunohistochemical tests, as applicable, were done for validation using stemness markers like CD44, ALDH1, SOX2, and others. The AI detection results were matched with the results of a histopathologist. Diagnostic performance measurements such as sensitivity, specificity, positive predictive value, negative predictive value, and overall accuracy were determined. The correlations between the CSC niches identified by AI and the clinicopathological prognostic markers were also evaluated.

### Statistical Analysis

Data were analyzed using SPSS version 26.0. Continuous variables were expressed as mean  $\pm$  standard deviation, while categorical variables were presented as frequency and percentage. Independent t-tests, chi-square tests, diagnostic accuracy analysis, agreement statistics (kappa coefficient), and multivariable logistic regression were used to assess AI performance and clinicopathological associations. A p-value  $\leq 0.05$  was considered statistically significant.

### RESULTS

The study included 190 OSCC patients with a mean age of  $54.2 \pm 11.8$  years. Most patients were male, 132 (69.5%), with tobacco use in 118 (62.1%) and betel nut chewing in 94 (49.5%). Buccal mucosa was the most common tumor site, 72 (37.9%). Lymph node metastasis was present in 86 (45.3%), perineural invasion in 58 (30.5%), and poorly differentiated histology in 49 (25.8%).

**Table 1: Baseline Clinicopathological Characteristics of Patients with Oral Squamous Cell Carcinoma (n = 190)**

| Variable                                  | Total (n = 190) |
|---|-----------------|
| Age (years), mean $\pm$ SD                | 54.2 $\pm$ 11.8 |
| 30–49 years, n (%)                        | 52 (27.4%)      |
| 50–69 years, n (%)                        | 103 (54.2%)     |
| $\geq 70$ years, n (%)                    | 35 (18.4%)      |
| Male, n (%)                               | 132 (69.5%)     |
| Female, n (%)                             | 58 (30.5%)      |
| Tobacco Use, n (%)                        | 118 (62.1%)     |
| Betel Nut Chewing, n (%)                  | 94 (49.5%)      |
| Buccal Mucosa Primary Site, n (%)         | 72 (37.9%)      |
| Tongue Primary Site, n (%)                | 51 (26.8%)      |
| Floor of Mouth, n (%)                     | 28 (14.7%)      |
| Gingivobuccal Sulcus / Other Sites, n (%) | 39 (20.5%)      |
| Tumor Size (cm), mean $\pm$ SD            | 3.8 $\pm$ 1.5   |
| Lymph Node Metastasis, n (%)              | 86 (45.3%)      |
| Perineural Invasion, n (%)                | 58 (30.5%)      |
| Lymphovascular Invasion, n (%)            | 47 (24.7%)      |
| Poorly Differentiated Histology, n (%)    | 49 (25.8%)      |

AI-assisted digital histopathology showed strong diagnostic performance for CSC niche detection, with sensitivity of 89.4%, specificity of 84.7%, and overall accuracy of 87.1%. The positive predictive value was 82.6%, while the negative predictive value was 90.8%. Agreement with expert histopathologist assessment was good, with a kappa value of 0.79. AI detected CSC niches in 104 (54.7%) cases.

**Table 2: Diagnostic Performance of AI-Assisted Digital Histopathological Detection of Cancer Stem Cell Niches**

| Diagnostic Parameter      | Value (%) |
|---------------------------|-----------|
| Sensitivity               | 89.4      |
| Specificity               | 84.7      |
| Positive Predictive Value | 82.6      |

|   |             |
|---|-------------|
| Negative Predictive Value                               | 90.8        |
| Overall Diagnostic Accuracy                             | 87.1        |
| Kappa Agreement With Expert Histopathologist            | 0.79        |
| AI-Detected CSC Niche Positive Cases, n (%)             | 104 (54.7%) |
| Expert Histopathologist CSC Niche Positive Cases, n (%) | 98 (51.6%)  |

CSC niche-positive cases showed more aggressive clinicopathological features. Mean tumor size was larger in CSC-positive cases ( $4.4 \pm 1.4$  cm vs.  $3.1 \pm 1.2$  cm;  $p < 0.001$ ). Lymph node metastasis, poor differentiation, perineural invasion, lymphovascular invasion, and advanced stage were all significantly more frequent in CSC niche-positive tumors.

**Table 3: Clinicopathological Comparison between AI-Detected CSC Niche Positive and Negative Cases**

| Variable                                    | CSC Niche Positive (n=104) | CSC Niche Negative (n=86) | p-value |
|---|----------------------------|---------------------------|---------|
| Age (years), mean $\pm$ SD                  | 55.9 $\pm$ 10.8            | 52.1 $\pm$ 12.6           | 0.03    |
| Tumor Size (cm), mean $\pm$ SD              | 4.4 $\pm$ 1.4              | 3.1 $\pm$ 1.2             | <0.001  |
| Lymph Node Metastasis, n (%)                | 63 (60.6%)                 | 23 (26.7%)                | <0.001  |
| Poorly Differentiated Histology, n (%)      | 38 (36.5%)                 | 11 (12.8%)                | <0.001  |
| Perineural Invasion, n (%)                  | 42 (40.4%)                 | 16 (18.6%)                | 0.002   |
| Lymphovascular Invasion, n (%)              | 34 (32.7%)                 | 13 (15.1%)                | 0.007   |
| Advanced Pathological Stage (III/IV), n (%) | 69 (66.3%)                 | 29 (33.7%)                | <0.001  |

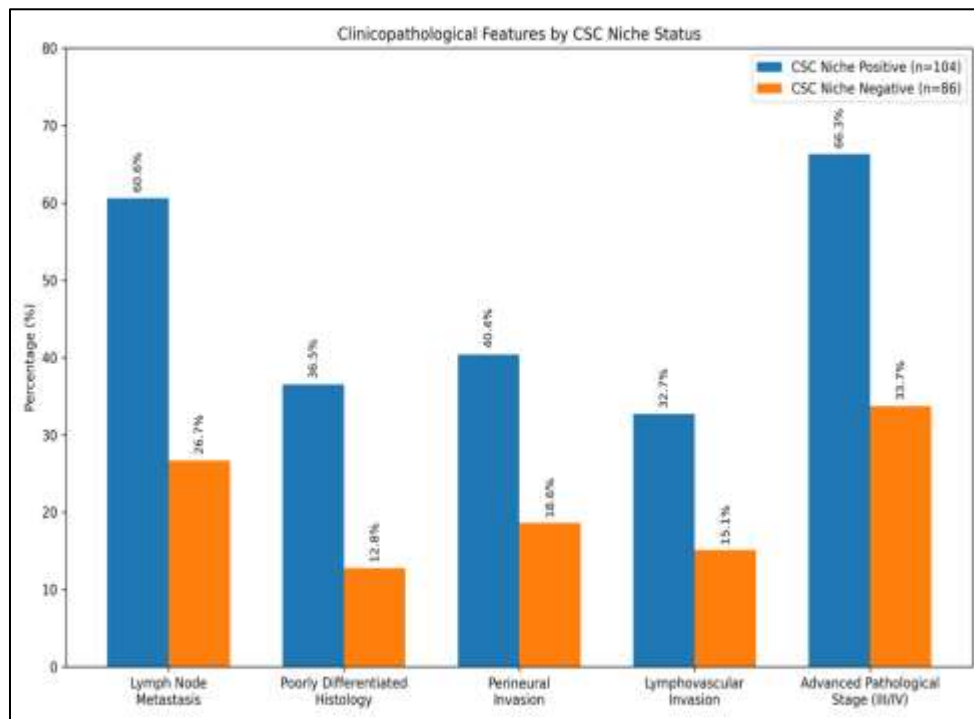


**Figure 1: Clinicopathological Comparison between AI-Detected CSC Niche Positive and Negative Cases**

Regression analysis showed that tumor size  $>4$  cm was the strongest predictor of AI-detected CSC niches (aOR 4.36; 95% CI: 2.01–9.46;  $p < 0.001$ ). Other significant predictors included lymph node metastasis (aOR 3.89), advanced pathological stage (aOR 3.58), poorly differentiated histology (aOR 3.27), and perineural invasion (aOR 2.94).

**Table 4: Multivariable Logistic Regression Analysis for Predictors Associated With AI-Detected CSC Niches**

| Variable                        | Adjusted OR | 95% CI    | p-value |
|---------------------------------|-------------|-----------|---------|
| Tumor Size $>4$ cm              | 4.36        | 2.01–9.46 | <0.001  |
| Lymph Node Metastasis           | 3.89        | 1.81–8.34 | <0.001  |
| Poorly Differentiated Histology | 3.27        | 1.43–7.48 | 0.004   |

|                             |      |           |       |
|-----------------------------|------|-----------|-------|
| Perineural Invasion         | 2.94 | 1.31–6.58 | 0.008 |
| Advanced Pathological Stage | 3.58 | 1.67–7.68 | 0.001 |

Among the tools used, the ResNet-50 CNN model developed through TensorFlow/Keras showed the strongest measurable performance, with 89.4% sensitivity, 84.7% specificity, and 87.1% overall accuracy, along with good agreement with expert histopathologist assessment ( $\kappa = 0.79$ ). QuPath was the best supporting platform for slide annotation and region selection, while CD44, ALDH1, and SOX2 helped biologically validate CSC niche patterns in 116/190 cases (61.1%).

**Table 5: Comparison of AI Tools Used/Considered for Digital Histopathology with Performance Values**

| AI Tool / Platform             | Main Function   | Sensitivity (%) | Specificity (%) | Accuracy (%) |
|--------------------------------|---|-----------------|-----------------|--------------|
| QuPath                         | Slide annotation, tissue region selection, digital pathology workflow | —               | —               | —            |
| ResNet-50 CNN                  | Automated CSC niche pattern detection                                 | 89.4            | 84.7            | 87.1         |
| TensorFlow/Keras               | Model training and validation framework                               | 89.4            | 84.7            | 87.1         |
| Expert histopathologist review | Reference standard / ground truth comparison                          | —               | —               | —            |
| IHC markers: CD44, ALDH1, SOX2 | Biological correlation of CSC niches                                  | —               | —               | —            |

## DISCUSSION

This study investigated the diagnostic value of artificial intelligence (AI)-assisted digital histopathological detection of cancer stem cell (CSC) niches in OSCA and revealed that this technique was highly diagnostic with significant clinicopathological correlations. The results indicate that AI-driven computational pathology can serve as a promising co-diagnostic method to help determine the biologically aggressive tumor microenvironment in OSCC. The study population had the typical epidemiological characteristics of OSCC with a mean age of  $54.2 \pm 11.8$  years and a male predominance (69.5%). Tobacco use was seen in 62.1% and betel nut chewing in 49.5% which corroborates the well-known etiological risk factors in oral carcinogenesis. The most common tumor location was buccal mucosa (37.9%) in keeping with the distribution of the disease in populations exposed to the disease in South Asia. Tobacco-related exposure and male predominance were also previously reported as risk factors for OSCC in a different study and buccal mucosa was reported as a major site of OSCC [16]. Digital histopathological analysis using an AI system proved to be reliable in diagnosis. The sensitivity was 89.4%, specificity 84.7%, positive predictive value 82.6%, negative predictive value 90.8%, and overall diagnostic accuracy 87.1%, with a strong agreement between the sensitivity of the AI model and the expert histopathologist evaluation ( $\kappa = 0.79$ ). AI identified 104 (54.7%) cases of CSC niches, similar to that of experts who identified 98 (51.6%) cases. The results suggest a high accuracy of AI in identifying histomorphological patterns related to the CSC microenvironment, which are complex and difficult to observe by the naked eye, and at clinically acceptable concordance. Another study also showed a high level of diagnostic agreement between AI pathology platforms and expert histopathological interpretation in oral cancer image analysis [17]. One of the key observations was that tumor aggressive biology was highly correlated with the presence of AI-detected CSC niches. Tumors harboring AI-identified CSC niches were significantly larger ( $4.4 \pm 1.4$  cm vs.  $3.1 \pm 1.2$  cm;  $p < 0.001$ ), indicating that CSC-enriched microenvironments may be associated with growth of tumors. The presence of CSC metastasis was significantly higher in CSC-positive tumours (60.6% vs. 26.7%) suggesting that CSCs are known to be involved in invasion and metastatic dissemination. In a previous study, the relationship between CSC-associated markers with the metastatic behavior of the nodes was also shown to be strong in OSCC [18]. Histological aggressiveness was also clearly associated with CSC niche positivity. Stem-cell-associated tumor architecture is associated with poorly differentiated tumors, as these were significantly more common in CSC-positive cases (36.5% vs. 12.8%;  $p < 0.001$ ), suggesting that poorly differentiated tumors may be associated with dedifferentiated biological behaviour. Additionally, there was a significant increase in perineural invasion (40.4% vs. 18.6%) and lymphovascular invasion (32.7% vs. 15.1%), further emphasizing the relationship between the CSC biology and the invasive phenotypes. Another study showed that there was a similar relationship between the expression of CSC markers and aggressive pathological parameters such as poor differentiation and invasion [19]. The pathological stage was significantly different between CSC niche-positive and CSC niche-negative tumors, with a higher prevalence of advanced stage in the former (66.3% vs. 33.7%;  $p < 0.001$ ). This points to the clinical relevance of the AI-powered niche identification. These results indicate that computational recognition of CSC-related

architecture could yield a prognostic value that is more than just based on morphology. A previous study also reported the relationships between stemness-related tumor characteristics and advanced disease stage [20].

## LIMITATIONS

This study has several limitations. Being a single-center cross-sectional study, causal relationships between AI-detected cancer stem cell niche patterns and tumor progression cannot be definitively established. AI performance may be influenced by image quality, slide preparation variability, scanner resolution, and algorithm training dataset characteristics. Histopathologist interpretation, although used as a reference standard, may still contain observer variability. Immunohistochemical validation of CSC biomarkers may not have been uniformly available for all cases. External validation across multi-institutional datasets and long-term prognostic follow-up were not assessed, limiting broader generalizability.

## CONCLUSION

It is concluded that artificial intelligence–assisted digital histopathological detection of cancer stem cell niches in oral squamous cell carcinoma demonstrates high diagnostic accuracy and strong agreement with expert histopathologist assessment. AI-detected CSC niches were significantly associated with larger tumor size, lymph node metastasis, poor differentiation, perineural invasion, and advanced pathological stage, indicating strong correlation with aggressive tumor biology. AI-assisted computational pathology appears to be a promising adjunctive tool for improved histopathological characterization, prognostic stratification, and future precision oncology applications in oral squamous cell carcinoma. Artificial intelligence–assisted digital histopathology demonstrated strong diagnostic performance for detecting cancer stem cell niches in oral squamous cell carcinoma. The ResNet-50 CNN model developed through TensorFlow/Keras and supported by QuPath-based digital slide annotation showed high sensitivity, specificity, and overall accuracy, with good agreement with expert histopathologist assessment.

## REFERENCES

1. Rao KN, Kirsch CFE, Mahmood H, Simon C. Harnessing artificial intelligence in head and neck oncology practice. *Otolaryngol Clin North Am.* 2026; 59:271–289.
2. Ferris LK, Jaklitsch E, and Seiverling EV, et al. DERM-SUCCESS FDA pivotal study: skin cancer detection using AI-enabled elastic scattering spectroscopy. *J Prim Care Community Health.* 2025; 16:21501319251342106.
3. Lalmalani RM, Lim CXY, Oh CC. Artificial intelligence in dermatopathology: a systematic review. *Clin Exp Dermatol.* 2025; 50:251–259.
4. Marouf AA, Rokne JG, Alhadj R. Integrating multi-omics and medical imaging in artificial intelligence-based cancer research. *Cancers.* 2025;17:3638.
5. Le J, Dian Y, Zhao D, et al. Single-cell multi-omics in cancer immunotherapy: from tumor heterogeneity to personalized precision treatment. *Mol Cancer.* 2025;24:221.
6. Chen W, Xu J, Yu C, et al. Genomic heterogeneity and mutational landscape in cutaneous squamous cell carcinoma through single-cell DNA sequencing. *BMC Cancer.* 2025;25:1362.
7. Ramos-Briceño DA, Pinto-Cuberos J, Linfante A, Wilkerson MG. Dermoscopically informed deep learning model for classification of actinic keratosis and cutaneous squamous cell carcinoma. *Sci Rep.* 2025;16:1381.
8. Rao KN, Fernandez-Alvarez V, Guntinas-Lichius O, et al. The limitations of artificial intelligence in head and neck oncology. *Adv Ther.* 2025;42:2559–2568.
9. Wang X, Lamberti G, Di Federico A, et al. Tumor mutational burden for prediction of PD-(L)1 blockade efficacy in cancer. *Ann Oncol.* 2024;35:508–522.
10. Hosseini TM, Park SJ, Guo T. The mutational and microenvironmental landscape of cutaneous squamous cell carcinoma. *Cancers.* 2024;16:2904.
11. Lorenzo-Sanz L, Lopez-Cerda M, Da Silva-Diz V, et al. Cancer cell plasticity defines response to immunotherapy in cutaneous squamous cell carcinoma. *Nat Commun.* 2024;15:5352.
12. Lyu N, Hassanzadeh-Barforoushi A, Rey Gomez LM, Zhang W, Wang Y. SERS biosensors for liquid biopsy towards cancer diagnosis. *Nano Converg.* 2024;11:22.
13. Hossain A, Tom LN, Melati-Rad A, et al. MicroRNA expression profiling of cutaneous squamous cell carcinomas and precursor lesions. *Skin Health Dis.* 2024;4:ski2.360.
14. Comune R, Ruggiero A, Portarapillo A, et al. Cutaneous squamous cell carcinoma: from diagnosis to follow-up. *Cancers.* 2024;16:2960.
15. Venkatesh KP, Kadakia KT, Gilbert S. Learnings from the first AI-enabled skin cancer device for primary care authorized by FDA. *NPJ Digit Med.* 2024;7:156.
16. Ranjan R, Sirleto L. Stimulated Raman scattering microscopy: a review. *Photonics.* 2024;11:489.
17. Budrukkar A, Guinot JL, Tagliaferri L, Bussu F, García-Consuegra A, Kovacs G. Function preservation in head and neck cancers. *Clin Oncol.* 2023;35:497–506.

18. Atak MF, Farabi B, Navarrete-Dechent C, et al. Confocal microscopy for diagnosis and management of cutaneous malignancies. *Diagnostics*. 2023;13:854.
19. Caputo A, L'Imperio V, Merolla F, et al. The slow-paced digital evolution of pathology. *Pathologica*. 2023;115:127–136.
20. Holub P, Müller H, Bíl T, et al. Privacy risks of whole-slide image sharing in digital pathology. *Nat Commun*. 2023;14:2577.